

A SEARCH FOR MILLION DEGREE GAS IN THE GALACTIC HALO AND THE LARGE
MAGELLANIC CLOUD THROUGH [Fe x] $\lambda 6375$ ABSORPTIONMAX PETTINI¹ AND SANDRO D'ODORICO
European Southern Observatory

Received 1986 February 18; accepted 1986 April 25

ABSTRACT

We have extended previous interstellar searches for the coronal forbidden line [Fe x] $\lambda 6374.51$ by obtaining echelle CCD spectra of two distant stars in the Galactic halo and two stars in the 30 Doradus H II region of the Large Magellanic Cloud. No [Fe x] absorption was detected, with 3σ upper limits as low as $4 \text{ m}\text{\AA}$, corresponding to $N(\text{Fe}^{9+}) \leq 5 \times 10^{16} \text{ cm}^{-2}$. The limits reached are comparable to the best achieved in earlier work, while referring to path lengths up to ~ 100 times longer. By considering these results together with other available data on highly ionized gas in the four directions studied, it is concluded that the detection limit apparently needs to be improved by about 1 order of magnitude in order to reach levels at which the [Fe x] observations can help discriminate between current theoretical models of the Galactic corona.

Among the weak interstellar features which we did detect near 6375 \AA are the diffuse interstellar bands (DIBs) $\lambda\lambda 6376.08, 6379.30$ in the LMC; this is the first time these features have been observed outside our Galaxy. We do not find their strength to be significantly enhanced relative to the Galactic relation with the color excess $E(B - V)$, as may have been expected from the fact that the LMC extinction curve shows a more pronounced far-ultraviolet rise than that produced by Galactic dust. However, we do find some indication that the relation between DIB equivalent widths and color excess may be modified in regions of low reddening.

Our echelle spectra also encompass the region of the Na I D doublet lines, which we have recorded with signal-to-noise ratios as high as ~ 250 . Toward the two halo stars we find evidence for clouds moving with Galactic rotation at distances of up to ~ 1.5 kpc below the plane, while the data for the two stars in 30 Doradus suggest the existence of a newly recognized shell, located *in front* of the H II region, and expanding with $v = 28 \text{ km s}^{-1}$ relative to the ambient medium.

Subject headings: galaxies: Magellanic Clouds — galaxies: structure — interstellar: abundances — interstellar: matter

I. INTRODUCTION

In a recent series of papers Hobbs (1984*a, b*, 1985) has raised the interesting possibility that interstellar gas at coronal temperatures ($T \gtrsim 10^6 \text{ K}$) may be detectable in absorption via forbidden optical lines, principally [Fe x] $\lambda 6374.51$. Despite the observational difficulties in registering extremely weak lines, with expected equivalent widths $W_\lambda \lesssim 1 \text{ m}\text{\AA}$, the incentives for such a search are considerable, as emphasized by Jenkins (1984). The prospects are still unclear for future space missions capable of accessing the resonance transitions of highly charged ions in the far-ultraviolet and soft X-ray ranges (York and Cowie 1983; Pettini and Boksenberg 1987); consequently, the visible coronal lines may be the only means at our disposal for several years for tracing the extent and distribution of very hot gas in the Galaxy. [Note, however, that with the Hubble Space Telescope it should be possible, in the near future, to look for the O VI $\lambda\lambda 1032, 1038$ doublet in QSO absorption line systems of sufficiently low redshift ($z_{\text{abs}} = 0.1-0.5$) that the intervening galaxies producing the absorption can be imaged relatively easily (see, for example, Bergeron 1986)].

The results of Hobbs's survey of [Fe x] $\lambda 6375$ published to date (Hobbs 1984*a, b*, 1985) consist of observations of this spectral region in a sample of 37 bright stars, located mostly in the disk within 1-2 kpc from the Sun, but also including a few

OB stars in the inner halo of the Galaxy, with distances from the plane of up to $z \approx 2.5$ kpc. In none of these directions was interstellar [Fe x] $\lambda 6375$ detected; the most stringent upper limits (3σ) achieved are $W_\lambda \lesssim 3 \text{ m}\text{\AA}$ for features of the thermal width appropriate to $T \approx 10^6 \text{ K}$ gas. This limit was set by detector instabilities (Hobbs used mainly a dual-array Digicon) and applies to the brightest stars in the sample; for the fainter halo stars typical 3σ upper limits are in the range $W_\lambda < 7-19 \text{ m}\text{\AA}$. Despite these negative results, there is a strong motivation to extend the search for [Fe x] $\lambda 6375$ to reach both more stringent detection limits and more distant regions of the Galaxy. This task is made easier by Hobbs's very careful study of this spectral region, which has provided essential information on a number of nearby telluric, interstellar, and stellar features and has shown that, once recognized, these should not in general pose serious problems.

In this paper we present the results of a search for interstellar [Fe x] $\lambda 6375$ absorption along very extended path lengths to two distant halo stars and to two stars in the 30 Doradus H II region in the Large Magellanic Cloud. As described in § II below, the observations were carried out with a CCD echelle spectrograph on the ESO 3.6 m telescope. Our data are an important extension of Hobbs's survey, for the following reasons. First, by taking advantage of the larger telescope aperture, and especially of the higher detective quantum efficiency and photometric stability of the CCD compared with the Digicon, we are able to reach signal-to-noise ratios compara-

¹ Also Royal Greenwich Observatory.

ble to the best achieved by Hobbs ($S/N \approx 350$), but over path lengths of up to ~ 50 kpc through the Galactic halo, as opposed to ~ 0.5 kpc through the disk. Second, along all three directions observed (considering here the two stars in 30 Dor together), absorption lines of highly ionized species dominant in gas at $T \approx 10^5$ K (Si iv, C iv, and N v) have been detected with the *International Ultraviolet Explorer* (*IUE*), at Galactic velocities and, for the 30 Dor sight line, also at LMC velocities (Pettini and West 1982; Savage and Massa 1985; Savage and de Boer 1981). These features have been generally interpreted as evidence for extended gaseous coronae around our Galaxy and possibly the LMC (York 1982; de Boer and Savage 1980). If this gas is produced by the cooling of a million degree phase of the interstellar medium flowing up from the disk, as in a Galactic fountain model (Bregman 1980), the four sight lines investigated here may well be among the most promising directions in which to search for intrinsically weak coronal lines. Furthermore, detection of [Fe x] in these directions would allow the column density of million degree gas to be compared directly with that of the cooler component studied with the *IUE*, with very important diagnostic possibilities for models of the Galactic corona (e.g., Bregman and Harrington 1986). Finally, the two stars in 30 Dor may allow a detection of [Fe x] local to this giant H II region, which has an unusually large number of very early type stars (Melnick 1985; Walborn 1984), includes an extended X-ray source which may be related to the combined effects of the stellar winds within the nebula, and is surrounded by several X-ray supernova remnants (Long, Helfand, and Grabelsky 1981; Walborn 1984).

II. OBSERVATIONS AND DATA REDUCTION

Table 1 lists relevant parameters of the target stars together with details of the observations. HD 156359 and CPD $-74^\circ 1569$ are two halo stars from the *IUE* survey by Pettini and West (1982), where references to the sources of stellar data are given. Both stars are located in the inner regions of the Galaxy (at galactocentric distances of 4.7 and 6.0 kpc, respectively), where interstellar absorption is known to be exceedingly strong (Savage and Massa 1985). R136a is the brightest member of the core of the 30 Dor cluster and is itself a multiple system consisting of at least eight stars (Weigelt and Baier 1985). The integrated spectral type given in Table 1 is from Walborn (1977); the V -magnitude is an estimate by Feitzinger *et al.* (1980) for the inner $2''$ diameter region (comparable to the slit size of our observations; see below). The color excess was deduced by Fitzpatrick and Savage (1984) from an extensive study of the extinction properties of the 30

Dor region; the heliocentric velocity is an uncertain measure by Feast (1961). For the distance to the LMC we have adopted the result of the recent reassessment by Reid and Strugnell (1986), based on a new determination of the absolute magnitude of RR Lyrae stars, which gives a distance modulus ($m - M$) = 18.35 ± 0.10 . The last object observed, star 11 in 30 Dor, is from the spectroscopic and photometric survey of stars in the nebula by Melnick (1985) and is located $\sim 1'$ (~ 13.5 pc) to the southeast of R136a.

The data were secured in the period 1985 April 2–4 with CASPEC, the echelle spectrograph of the ESO 3.6 m telescope. The instrument has been described by D'Odorico and Tanné (1984). In its standard configuration it uses a 31.6 lines mm^{-1} echelle grating with a 300 lines mm^{-1} grating cross-disperser. The detector is a thinned, back-illuminated RCA CCD chip (type SID EX501), consisting of 512×320 square pixels, $30 \mu\text{m}$ in size. One echelle spectrum of each star was obtained, covering approximately 900 Å centered at 6100 Å (6200 Å for CPD $-74^\circ 1569$). With a spectrograph slit $1''.8$ wide (corresponding to 1.5 pixels at the detector) and exposure times of 30–60 minutes, between $\sim 40,000$ and $\sim 210,000$ counts per resolution element ($= 1.8$ pixels) were obtained near 6375 Å (see last two columns of Table 1). For each stellar spectrum, accompanying calibration exposures of a Th-Ar emission-line lamp (for wavelength reference) and of a continuum lamp (for flat-fielding) were obtained with the same instrumental setup and at the same telescope position as the stellar observations.

The spectra were extracted, reduced, and calibrated with the echelle data reduction package implemented within MIDAS, the image processing system developed at ESO for the VAX 11/780 computer (Ponz, Brinks, and D'Odorico 1986). The major steps in the reduction procedure have been described by D'Odorico, Pettini, and Ponz (1985). Analysis of the comparison Th-Ar emission-line spectra showed that the data have a resolution $\Delta v = 17 \text{ km s}^{-1}$ (FWHM), which is well suited to the present purposes, since any [Fe x] absorption produced in gas at $T = 10^5$ K is expected to have a minimum width $\delta v = 28 \text{ km s}^{-1}$ from thermal broadening alone. The wavelength accuracy of the spectra was measured to be $\pm 1\text{--}2 \text{ km s}^{-1}$. In the final step of the reduction, spectral regions of interest in the extracted echelle orders were normalized by fitting a number of splines to nearby "continuum windows," that is, portions of the spectra, outside the interstellar absorption lines being investigated, which were judged to be free of contaminating stellar and telluric features. A by-product of the continuum-fitting process is an empirical measure of the signal-to-noise ratio appropriate to the wavelength region

TABLE 1
RELEVANT DATA FOR THE STARS OBSERVED

Star (1)	l (2)	b (3)	MK Type (4)	V (mag) (5)	$E(B - V)$ (mag) (6)	d (kpc) (7)	z (kpc) (8)	v_{STAR}^a (km s^{-1}) (9)	Exposure (minutes) (10)	Total Counts (11)
HD 156359	328°7	−14°5	O9 III	9.67	0.17	9.0	−2.2	− 83	30	180,600
CPD $-74^\circ 1569$	317°0	−18°7	O9.5 V	10.15	0.14	5.6	−1.8	−134	45	180,600
R136a	279°4	−31°7	OB(n) + WN5–A(B)	10.77	0.34	47	−25	+236:	45	210,700
30 Dor No. 11	279°4	−31°7	B0.5 Ia	13.1	0.39	47	−25	?	60	38,100

^a All velocities in the paper are referred to the local standard of rest, unless otherwise stated.

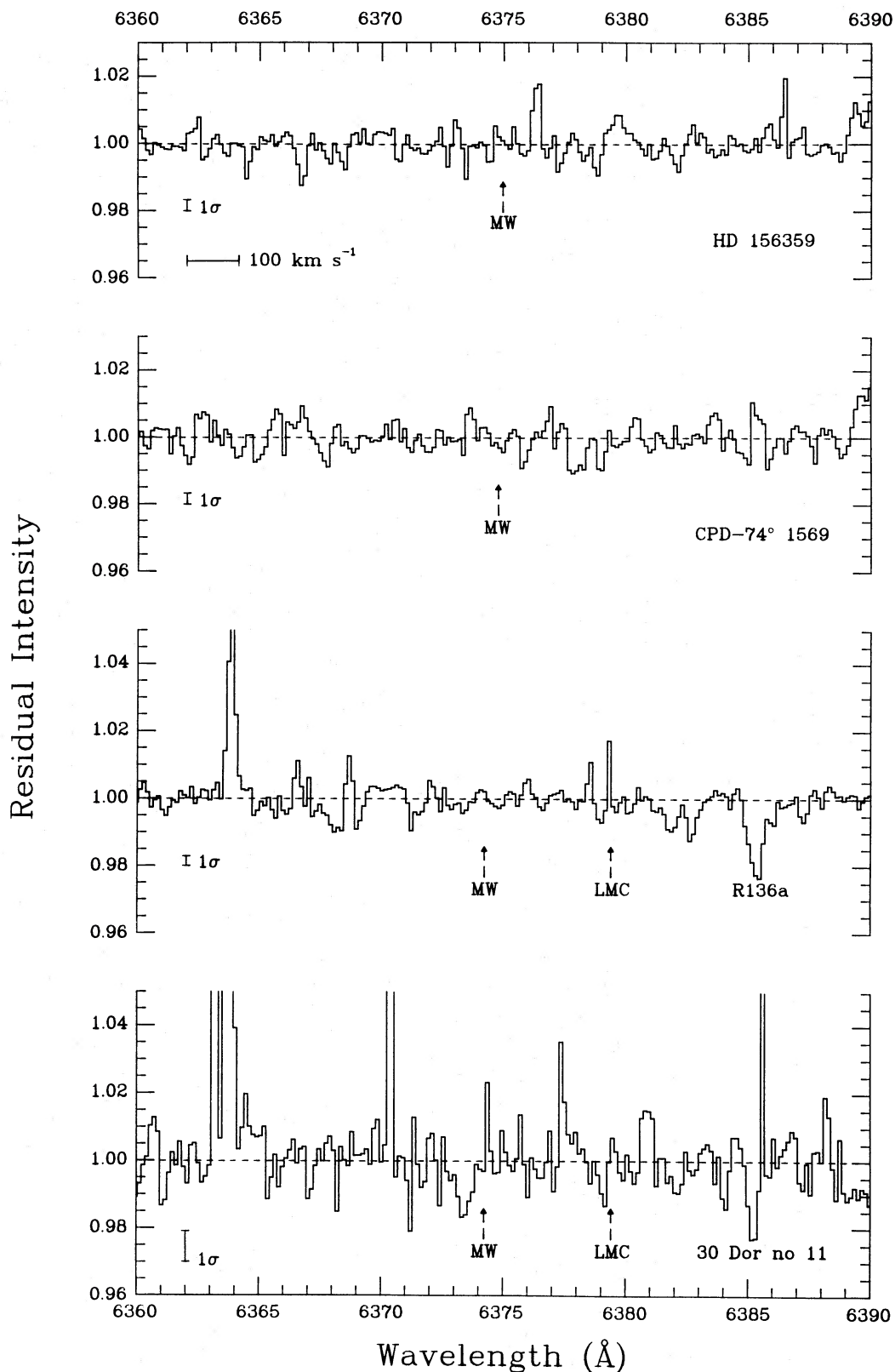


FIG. 1.—Portions of the spectra of the four stars observed encompassing the region of the [Fe x] $\lambda 6374.51$ line. Each spectrum has been normalized to the continuum level shown by the dashed horizontal line; the measured rms deviation of the data points about this level is indicated by the vertical bar labeled 1σ . Note the greatly expanded scale of the ordinates. The dashed arrows point to the approximate positions where [Fe x] absorption by gas in the Milky Way and the Large Magellanic Cloud may be expected to be found ($v_{\text{LSR}}=0$ and $v_{\text{LSR}}=+220$ km s⁻¹, respectively). No [Fe x] features are detected, with 3σ upper limits for the equivalent width as low as $W_{\lambda}^{\text{eq}}(3\sigma)=3.2$ mÅ (see Table 2). However, a number of weak stellar and interstellar lines are present, including the unidentified interstellar feature $\lambda 6367.25$ in HD 156359 ($\lambda_{\text{OBS}}=6366.71$ Å); possibly stellar N iv $\lambda 6380.77$ in CPD - 74°1569 ($\lambda_{\text{OBS}}=6378.01$ Å); and the diffuse interstellar bands $\lambda\lambda 6376.08, 6379.30$ in R136a at the velocity of neutral LMC gas, $v_{\text{LSR}}=+269$ km s⁻¹ ($\lambda_{\text{OBS}}=6382.18$ and $\lambda_{\text{OBS}}=6385.33$ Å, respectively). To our knowledge, this is the first detection of these features outside our Galaxy. The emission line visible in the two lower panels is [O I] $\lambda 6363.776$ from the night sky.

observed, $S/N = 1/\Delta I$, where ΔI is the rms deviation from the fitted continuum level of all the data points within the continuum windows.

III. RESULTS

a) [Fe x]

Figure 1 is a montage of the spectral region encompassing [Fe x] $\lambda 6374.51$ in the four stars observed and shows that *no [Fe x] absorption was detected in any of these directions*. In the figure, dashed arrows labeled *MW* point to the expected locations of any [Fe x] features centered at $v_{\text{LSR}} = 0 \text{ km s}^{-1}$ and thus likely to be due to local Milky Way gas. For comparison the *IUE* observations discussed below show that in the directions of HD 156359, CPD $-74^\circ 1569$, and 30 Dor, absorption by highly ionized species (C IV and N V) in the Galactic halo is strongest at $v_{\text{LSR}} = -30, -20,$ and 0 km s^{-1} , respectively (Pettini and West 1982; Savage and de Boer 1981). Similarly, the positions of the arrows labeled *LMC* in the two lower panels of Figure 1 correspond to $v_{\text{LSR}} = +220 \text{ km s}^{-1}$, where absorption by LMC highly ionized gas in front of 30 Dor is most pronounced (de Boer, Koornneef, and Savage 1980; K. S. de Boer and E. L. Fitzpatrick 1986, private communication).

Also indicated in each panel of Figure 1 is the measured rms deviation from the continuum level shown; the corresponding values of the signal-to-noise ratios achieved by these observations are listed in column (2) of Table 2. Comparison with the total number of counts *per resolution element* listed in the last column of Table 1 shows that for the three best exposed spectra we approach very closely the limit to the photometric accuracy set by the photon statistics. This implies negligible contributions to the final noise in the spectra by the readout noise of the RCA CCD chip (which is not surprising, since the signal recorded in each pixel generally greatly exceeded the square of the readout noise of $\sim 50e^-$ rms), and also by the uncertainty in the sensitivity calibration of the detector. Thus, the data presented here demonstrate that the pixel-to-pixel variations in the response of this RCA CCD chip, including fringing at the 5%–10% level, can indeed be corrected with an accuracy significantly better than 0.5% of the signal. For the

fourth, and faintest, of the stars observed (30 Dor No. 11), the signal-to-noise ratio measured is only about three-quarters of the limit set by the photon statistics, probably as a result of the greater proportional contribution of the readout noise to this more weakly exposed spectrum (see col. [11] of Table 1).

Returning to [Fe x], columns (3) and (4) of Table 2 give the 3σ upper limits to the equivalent width of absorption features, based on the measured signal-to-noise ratios listed in column (2). Following Hobbs (1984a), we give both $W_\lambda^d(3\sigma)$, the detection limit for narrow features with the instrumental width $\Delta v = 17 \text{ km s}^{-1}$, and $W_\lambda^{\text{th}}(3\sigma)$, the upper limit for broader absorption lines of width $\delta v = 30 \text{ km s}^{-1}$, expected from thermal broadening alone at $T \approx 10^6 \text{ K}$. The most sensitive [Fe x] upper limit achieved, $W_\lambda^{\text{th}}(3\sigma) \leq 4.2 \text{ m\AA}$ toward R136a, is comparable to the best limits reached in Hobbs's (1984a) survey, $W_\lambda^{\text{th}}(3\sigma) \leq 2.9 \text{ m\AA}$, while referring to a path length ~ 100 times longer. Column (5) lists the upper limits to the column density of Fe^{9+} corresponding to the values of $W_\lambda^{\text{th}}(3\sigma)$, adopting a value of the oscillator strength for the transition of $f = 2.1 \times 10^{-7}$ (Hobbs 1984b and references therein). In columns (6) and (7) of Table 2 we have collected the best available measurements of the corresponding column densities of C^{3+} and N^{4+} in the four directions, as referenced in the table. The values for HD 156359 from the analysis by Pettini and West (1982) are in good agreement with the independent estimates by Savage and Massa (1985). The values for CPD $-74^\circ 1569$ are from unpublished spectra of improved signal-to-noise ratios achieved by adding together several *IUE* images.

In the last three columns of Table 2 we give the total column densities of highly ionized gas implied, respectively, by the Fe^{9+} , C^{3+} , and N^{4+} column densities, assuming (a) solar abundances (Withbroe 1971) and (b) that the ions observed trace gas at temperatures where their fractional abundances peak in collisional equilibrium (respectively, $T_{\text{MAX}} = 1.25 \times 10^6, 1.0 \times 10^5,$ and $1.75 \times 10^5 \text{ K}$, where $\text{Fe}^{9+}, \text{C}^{3+},$ and N^{4+} are calculated to constitute 0.26, 0.34, and 0.23 of the total amounts of Fe, C, and N; Shull and van Steenberg 1982). Note from Table 2 that the column densities of gas at $T \approx 10^5 \text{ K}$ implied by the N v doublet, when detected, are lower than

TABLE 2
[Fe x] DETECTION LIMITS AND COLUMN DENSITIES OF HIGHLY IONIZED GAS

Star (1)	S/N (2)	$W_\lambda^d(3\sigma)$ (mÅ) (3)	$W_\lambda^{\text{th}}(3\sigma)$ (mÅ) (4)	$N(\text{Fe}^{9+})$ (10^{16} cm^{-2}) (5)	$N(\text{C}^{3+})$ (10^{13} cm^{-2}) (6)	$N(\text{N}^{4+})$ (10^{13} cm^{-2}) (7)	$N_{\text{H}}(\text{Fe}^{9+})^a$ (10^{21} cm^{-2}) (8)	$N_{\text{H}}(\text{C}^{3+})^b$ (10^{17} cm^{-2}) (9)	$N_{\text{H}}(\text{N}^{4+})^b$ (10^{17} cm^{-2}) (10)
Milky Way Gas									
HD 156359	300	3.6	4.8	≤ 6.3	$\geq 50^e$	8^e	≤ 9.6	≥ 40	30
CPD $-74^\circ 1569$	300	3.6	4.8	≤ 6.3	$> 15^d$	0.7^d	≤ 9.6	> 12	2.5
R136a	340	3.2	4.2	≤ 5.6	8^e	$\leq 3^f$	≤ 8.5	6	≤ 12
30 Dor No. 11	105	10.3	13.7	≤ 18	8^e	$\leq 3^f$	≤ 28	6	≤ 12
LMC Gas									
R136a	340	3.2	4.2	≤ 5.6	$> 20^g$...	≤ 8.5	> 16	...
30 Dor No. 11	105	10.3	13.7	≤ 18	≤ 28

^a Total column density of gas at $T \approx 10^6 \text{ K}$ implied by the column density of Fe^{9+} .

^b Total column density of gas at $T \approx 10^5 \text{ K}$ implied by the column densities of C^{3+} and N^{4+} , respectively.

^c Pettini and West 1982.

^d West and Pettini, unpublished.

^e Savage and de Boer 1981.

^f Savage 1985.

^g De Boer, Koornneef, and Savage 1980.

those suggested by the corresponding C IV measurements. A plausible explanation for this is that photoionization (by diffuse starlight and the extragalactic EUV and soft X-ray background) is an additional, and perhaps the dominant, production mechanism for C^{3+} ions in the Galactic halo, as considered in a number of recent analyses (Hartquist, Pettini, and Tallant 1984; Fransson and Chevalier 1985; Savage and Massa 1985; Bregman and Harrington 1986). On the other hand, photoionization is likely to be less important for N^{4+} , owing to the higher ionization potential which lies beyond the He II edge in stellar spectra at 54 eV (77.5 eV are required to convert N^{3+} to N^{4+}). Assuming that N^{4+} and Fe^{9+} are both produced in collisional ionization equilibrium, we see from columns (10) and (8) of Table 2 that, in the most favorable case (HD 156359), the upper limit on the column density of million degree gas implied by our [Fe x] observations exceeds by about 3 orders of magnitude the column density of gas at $T \approx 10^5$ K detected in N v.

In order to assess the significance of this, we have to consider the relative amounts of gas which we would expect to find at $T \approx 10^6$ K and $T \approx 10^5$ K. If the gas is initially heated to very high temperatures and then cools radiatively in pressure equilibrium, the cooling time is proportional to $T^{5/2}$, since the cooling function Λ is proportional to $T^{-1/2}$ over the interval $5 \leq \log T \leq 7$ (Kahn 1976). Furthermore, since the temperature profiles of the Fe^{9+} and N^{4+} fractional abundance curves are of similar widths about their respective peaks at $T_{MAX} = 1.25 \times 10^6$ and $T_{MAX} = 1.75 \times 10^5$ K (Shull and van Steenberg 1982), it follows that, to a first approximation, the column densities of the hot gas traced by these two ions can also be taken to be proportional to $T_{MAX}^{5/2}$. Consequently, we would expect the column density of million degree gas producing [Fe x] absorption to be ~ 150 times higher than that of the cooler phase responsible for the N v lines. (If the gas cools isochorically, rather than in pressure equilibrium, the temperature decrease is faster over the range considered here, and a time-dependent analysis is required to calculate the resulting ion fractions, since the gas cools more rapidly than it can recombine). An alternative possibility is that the high ions in the halo are formed at the conductive interfaces of cool clouds in pressure equilibrium with a surrounding hot Galactic corona, as in the picture originally suggested by Spitzer (1956); the cool clouds may be condensations within a Galactic fountain (Bregman 1980). In this case, the calculations by McKee and Cowie (1977) show that the column density of gas within a given (logarithmic) temperature range across the evaporative cloud surface is proportional to $T^{2.05}$. Thus, we would expect

approximately 50 times more gas at the temperatures traced by Fe^{9+} than in the cooler zone where N^{4+} ions are most abundant.

In conclusion, then, although the [Fe x] observations presented here are a substantial extension of previous searches for this line, they still fall short by about 1 order of magnitude of the sensitivity apparently required to detect the million degree phase of the interstellar medium, at least on the basis of current theoretical models of the Galactic corona. On the other hand, the work of Savage and Massa (1985) has revealed a number of bright stars near the Galactic center where $N(N^{4+}) \gtrsim 1 \times 10^{14} \text{ cm}^{-2}$; in these directions it should be possible with CCDs to push the detection limit of [Fe x] $\lambda 6375$ nearer levels of diagnostic value for different models of the corona.

Finally, we note that no [Fe x] absorption was found at LMC velocities either (see Fig. 1 and Table 2). The upper limit deduced, however, is no more instructive than those appropriate to Galactic gas, since N v absorption in front of 30 Dor does not appear to be unusually strong. Although no values of $N(N^{4+})$ in line to R136a have been published, the co-added spectra by de Boer, Fitzpatrick, and Savage (1985) suggest $N(N^{4+}) \leq 2 \times 10^{13} \text{ cm}^{-2}$ (K. S. de Boer and E. L. Fitzpatrick 1986, private communication), with some uncertainty because of blending with Galactic Mg II $\lambda 1239.925$. Toward HD 36402, ~ 1.5 from R136a, de Boer and Nash (1982) find $N(N^{4+}) = 3 \times 10^{13} \text{ cm}^{-2}$, but conclude that much of this gas could originate in a local superbubble.

b) Other Absorption Lines

Although the search for [Fe x] yielded negative results, we did detect a number of weak interstellar and stellar absorption lines in the wavelength region near 6375 Å shown in Figure 1; their equivalent widths, with 1 σ errors, and central velocities are collected in Table 3. As well as being of intrinsic interest, these features, because of their small equivalent widths ($W_\lambda \approx 3.5\text{--}15.5 \text{ mÅ}$), demonstrate further the high signal-to-noise ratios achieved in these observations and confirm the corresponding 3 σ upper limits given in Table 2. We now discuss them briefly in turn.

i) The Unidentified Interstellar Feature $\lambda 6367.25$

Hobbs (1985) discovered this feature in the spectra of four reddened [$E(B - V) = 0.32\text{--}0.72$] stars observed in the course of his [Fe x] survey and concluded that it arises in cold, diffuse interstellar clouds and that it is either a molecular transition or a very weak diffuse interstellar band. Our spectrum of the moderately reddened star HD 156359 [$E(B - V) = 0.17$]

TABLE 3
STELLAR AND INTERSTELLAR ABSORPTION LINES DETECTED NEAR 6375 Å^a

STAR (1)	FEATURE UNIDENTIFIED IS $\lambda 6367.25$		DIB $\lambda 6376.08$		DIB $\lambda 6379.30$		STELLAR N IV $\lambda 6380.77$	
	W_λ (mÅ)	v_{LSR} (km s ⁻¹)	W_λ (mÅ)	v_{LSR} (km s ⁻¹)	W_λ (mÅ)	v_{LSR} (km s ⁻¹)	W_λ (mÅ)	v_{LSR} (km s ⁻¹)
HD 156359	4.1 ± 1.2	-5
CPD -74°1569	3.6 ± 1.2	-2	(7.6 ± 1.2)	(-118)
R136a	12.4 ± 1.7	+273:	15.7 ± 1.1	+269
30 Dor No. 11	9.5 ± 3 ^b	+264

^a In cases where no detection is reported, the 3 σ upper limits W_λ^u given in Table 2 apply to narrow features (FWHM = 0.36 Å).

^b Possibly blended with stellar N IV $\lambda 6379.62$.

indeed shows an absorption line at the $\sim 3.5 \sigma$ significance level centered at $\lambda_{\text{LSR}} = 6367.15 \text{ \AA}$ ($\lambda_{\text{OBS}} = 6366.71 \text{ \AA}$; see top panel of Fig. 1). The resulting value $v_{\text{LSR}} = -5 \text{ km s}^{-1}$ is sufficiently close to the velocity of the strongest Na I component in this direction ($v_{\text{LSR}} = 0 \text{ km s}^{-1}$; see § IV below) to make the identification highly plausible. Forcing an agreement with the Na I velocity would imply a laboratory wavelength for the feature of $\lambda_{\text{LAB}} = 6367.15$. With an equivalent width $W_{\lambda} = 4.1 \pm 1.2 \text{ m\AA}$, this is the lowest level at which this interstellar line has been detected to date, consistent with the lower reddening of HD 156359 compared with the disk stars in which Hobbs discovered the feature. The measured width of the absorption, $\text{FWHM} = 0.36 \pm 0.07 \text{ \AA}$, shows it to be unresolved in the present data; this is apparently in contrast with Hobbs's (1985) finding that the feature may be intrinsically broad and possibly consist of three components at 6366.97, 6367.21, and 6367.51 \AA .

ii) *The Diffuse Interstellar Bands $\lambda\lambda 6376.08, 6379.30$*

These two features have been studied extensively by Herbig (1975) and detected by Hobbs (1984a) in several reddened directions in the [Fe x] survey. They constitute a pair of a type which is not uncommon among diffuse interstellar bands, the feature at the longer wavelength being narrower, and generally stronger, than the shorter wavelength member, which is broad and shallow. Fourteen such pairs were identified by Herbig. The DIB $\lambda 6379.30$ appears to be present in CPD $-74^{\circ}1569$ at the 3σ level and at $v_{\text{LSR}} = -2 \text{ km s}^{-1}$ ($\lambda_{\text{OBS}} = 6378.99 \text{ \AA}$); in HD 156359 a weaker feature, with $W_{\lambda} = 3.0 \pm 1.2 \text{ m\AA}$, may also be $\lambda 6379.30$ at $v_{\text{LSR}} = -3 \text{ km s}^{-1}$, although we have not included it in Table 3 because its significance is only 2.5σ . By far the clearest, and most interesting, detection of the two diffuse bands, however, is at $v_{\text{LSR}} = +269 \text{ km s}^{-1}$ ($\lambda_{\text{OBS}} = 6382.18$ and $\lambda_{\text{OBS}} = 6385.33 \text{ \AA}$, respectively) in R136a (see third panel of Fig. 1). The velocity is in excellent agreement with that of the strongest component of lines from neutral gas in the LMC, as determined from both optical (Blades 1980; Walborn 1980; see also § IV below) and ultraviolet (de Boer, Fitzpatrick, and Savage 1985) observations, making this the first detection (to our knowledge) of these diffuse interstellar bands in an external galaxy. The DIB $\lambda 6379.30$ is sufficiently strong to be also detectable, at $v_{\text{LSR}} = +264 \text{ km s}^{-1}$, in 30 Dor No. 11 (see bottom panel of Fig. 1) for which the photometric accuracy achieved is worse than for R136a.

It is well known that the origin of the diffuse interstellar bands is an outstanding astrophysical puzzle, even though it is more than half a century since they were first recognized by Merrill (1934). Opinions are divided not only as to the identity of the carrier(s), but also as to whether the 45 currently known bands, of largely different widths and profiles, have a common source or not (e.g., Herbig 1975; Wu, York, and Snow 1981). Stable, long-chain carbon molecules (e.g., Crawford, Tielens, and Allamandola 1985; Kroto *et al.* 1985) and resonantly absorbing impurities in interstellar grains (e.g., Shapiro and Holcomb 1986) are recent formulations of the two classes of absorbers (free molecules and solid grains) which have traditionally been proposed as the band carriers.

In principle, our detection of the $\lambda\lambda 6376.08, 6379.30 \text{ \AA}$ features in the LMC may offer fresh information in the quest for their origin, since dust in the LMC has significantly different extinction properties from dust in the Milky Way (Nandy 1984). In practice, however, firm conclusions are hampered by two facts: (a) studies of possible correlations between diffuse

band strengths (and profiles) and details of the extinction curve have yielded divergent clues (e.g., Herbig 1975; Wu, York, and Snow 1981; Snow, Timothy, and Saar 1982; Seab and Snow 1984), and (b) differing interpretations have been put forward for the differences in the extinction curves of the Galaxy and the LMC (e.g., Koornneef and Code 1981; Bromage and Nandy 1983; de Boer 1984). Notwithstanding these difficulties, it is still instructive to consider what conclusions can be drawn from the observed strengths of the 6376.08, 6379.30 \AA bands in front of 30 Dor, since previous detections of diffuse bands in the LMC have been limited to broader features, principally $\lambda 4428$ (Blades and Madore 1979; Houziaux, Nandy, and Morgan 1980; Hutchings 1980), which inevitably suffers from blending with stellar lines and is thus difficult to measure precisely.

In his detailed study, Herbig (1975) found that, in the Galaxy, the strengths of the diffuse bands generally correlate well with the color excess $E(B - V)$ and put forward arguments in favor of the carrier of the lines being associated with the very small interstellar grains (with radius of a few hundred angstroms) responsible for the far-ultraviolet extinction. Grains of this size have also been shown by Welter and Savage (1977) to be required in order to reproduce the high degree of symmetry of $\lambda 6379.30$, if this feature is due to purely electronic transitions in grain impurities. On the basis of Herbig's correlations, our observed equivalent widths of $\lambda\lambda 6376.08, 6379.30$ in R136a would correspond to $E(B - V) = 0.12$ and $E(B - V) = 0.09$, respectively. The characteristics of the interstellar extinction in line to the 30 Dor H II region in general and to R136a in particular have been discussed extensively by Fitzpatrick and Savage (1984), who identified three distinct contributors to the overall extinction: Galactic foreground dust [$E(B - V) = 0.06$], LMC foreground dust [$E(B - V) = 0.11$], and 30 Dor nebular dust [$E(B - V) = 0.17$ toward R136a]. These three types of dust produce significantly different ultraviolet extinction curves, both in the strength of the 2175 \AA bump and in the far-ultraviolet rise. Relative to the standard Galactic reddening curve, the latter is respectively greatly enhanced and somewhat reduced in the widespread LMC dust and the nebular dust local to 30 Dor. The 2175 \AA bumps in both LMC curves are 20%–30% weaker, relative to $E(B - V)$, than the bump produced by Galactic dust. Relating these properties to the strength of the diffuse interstellar bands we have detected, the following points emerge.

1. Nebular dust is apparently relatively inefficient in producing diffuse interstellar bands. A similar effect is seen in some regions of the Galaxy with abnormally low far-ultraviolet extinction, most notably the ρ Oph dark cloud, where the diffuse bands are found to be systematically weaker (Snow and Cohen 1974; Herbig 1975). This is consistent with the viewpoint that the band carriers are small interstellar grains, since the reduced extinction in the far ultraviolet can be attributed to a shift in the particle-size distribution toward larger sizes (Mathis and Wallenhorst 1981).

2. On the other hand, the strength of $\lambda\lambda 6376.08, 6379.30$ in R136a does not appear to reflect the enhanced far ultraviolet extinction of LMC dust, since the observed equivalent widths match well the values expected for $E(B - V) = 0.11$ on the basis of Herbig's correlations, which refer to Galactic dust. A possible explanation of this is that the pronounced far-ultraviolet rise of the LMC extinction curve does not reflect a different distribution of grain sizes, with a greater proportion of small grains relative to Galactic dust, but rather results from

a reduction in the contribution to the extinction by graphite grains relative to silicates, as suggested by Bromage and Nandy (1983). An association of the carrier of the $\lambda 4428$ band with the dust component responsible for producing the 2175 Å bump, usually identified with graphite grains, has been proposed by Seab and Snow (1984), who found a weak, but significant, correlation between these two diffuse features. However, the weakness of the 2175 Å bump in the LMC and 30 Dor extinction curves, by only 20%–30% relative to the Galactic case, is perhaps insufficient to explain, by itself, the fact that the observed equivalent widths of $\lambda\lambda 6376.08, 6379.30$ are ~ 3 times smaller than expected on the basis of Herbig's results.

3. An alternative (or additional) possibility is that Herbig's correlations, which were derived from observations of heavily reddened stars, do not extrapolate to low values of $E(B - V)$ ($=0.1$ – 0.2). This seems to be suggested also by the relative weakness of the features $\lambda\lambda 6376.08, 6379.30$ in the two halo stars we observed, where $\lambda 6379.30$ is 4–5 times weaker than in R136a, although $E(B - V) \approx 0.15$. Perhaps the strengths of the diffuse interstellar bands are also dependent on the average reddening per unit distance. Smith *et al.* (1981) found a similar effect for the $\lambda 6195.95$ band, which in stars with $E(B - V) \lesssim 0.1$ is more than 1 order of magnitude weaker than expected from its dependence on color excess in more reddened stars. This result, which is reminiscent of the sharp $E(B - V)$ threshold for detection of H_2 (Spitzer, Cochran, and Hirshfeld 1974), was interpreted by Smith *et al.* (1981) as evidence for a molecular origin of the diffuse feature $\lambda 6195.95$ (see also Krishna Kumar, Federman, and Vanden Bout 1982).

iii) Stellar Lines

The spectral types of the four stars observed were chosen to minimize possible interference with any [Fe x] absorption by neighboring stellar features. The only stellar line we may have detected is N IV $\lambda 6380.77$ in CPD $-74^\circ 1569$ ($\lambda_{\text{OBS}} = 6378.01$ Å), but its strength ($W_\lambda = 7.6 \pm 1.2$ mÅ) appears somewhat high for the late-O type of star. Furthermore, its velocity ($v_{\text{LSR}} = -118$ km s $^{-1}$) does not agree as well as might be expected with the published value for CPD $-74^\circ 1569$ ($v_{\text{STAR}} = -134$ km s $^{-1}$), which is confirmed by our own observations of He I $\lambda 5875.63$ in the spectrum (see Table 4),

although the discrepancy may be due to noise interfering with this weak line (see Fig. 1). The feature at $\lambda_{\text{OBS}} = 6373.40 \pm 0.07$ Å in 30 Dor No. 11, with $W_\lambda = 11.0 \pm 3.5$ mÅ, is also likely to be stellar; an interstellar origin appears excluded by the fact that a corresponding absorption is absent in the spectrum of R136a (separated by only $\sim 1'$), which has a signal-to-noise ratio ≥ 3 times higher. However, we have not been able to find a likely identification for the line, partly because the radial velocity of the star is not known. At the average velocity of the stars in 30 Dor ($v_{\text{LSR}} = +245$ km s $^{-1}$), the laboratory wavelength of the line would be $\lambda_{\text{LAB}} = 6367.91 \pm 0.07$ Å; however, Hobbs's (1984a) analysis of this spectral region in OB stars apparently did not locate any stellar features of the requisite strength at, or near, this wavelength.

IV. Na I ABSORPTION

The echelle spectra obtained for the purpose of searching for [Fe x] absorption cover approximately 900 Å and therefore include a number of other features of interest. Here we consider briefly the interstellar Na I doublet lines ($\lambda\lambda 5889.950, 5895.924$), because in two cases (HD 156359 and 30 Dor No. 11) the data have not been published before and in the other two directions our observations have signal-to-noise ratios much superior to those of data in the literature. Normalized profiles of the Na I lines are reproduced in Figure 2; Table 4 gives relevant measurements, including the signal-to-noise ratios in this spectral region, and the central velocities and equivalent widths, together with the formal 1σ errors, of the different absorption components detected. Measurements of the stellar He I $\lambda 5875.63$ line in the two halo stars are also included. Comparison of the values in columns (2) of Tables 4 and 2 shows that the signal-to-noise ratios achieved at Na I are generally inferior to those measured near [Fe x]. This is due in part to the fact that the Na I lines were recorded in a region where the echelle blaze, optimized for [Fe x] $\lambda 6375$, is not at peak. Furthermore, the estimates of S/N given in Table 4 are probably somewhat pessimistic, since the rms deviations from the continuum level from which they were measured are likely to include several weak telluric water vapor lines which contaminate the Na I region. Only the strongest and most obvious

TABLE 4
ABSORPTION LINES IN THE Na I REGION

STAR (1)	S/N (2)	IS Na I D ₂		IS Na I D ₁		STELLAR He I $\lambda 5875.63$	
		W_λ (mÅ) (3)	v_{LSR} (km s $^{-1}$) (4)	W_λ (mÅ) (5)	v_{LSR} (km s $^{-1}$) (6)	W_λ (mÅ) (7)	v_{LSR} (km s $^{-1}$) (8)
HD 156359	220	253 \pm 2	+1	140 \pm 2	-0.5	1147 \pm 5	-72
		90 \pm 2	-37	52 \pm 2	-37		
		40 \pm 2	-81	16 \pm 2	-79		
CPD $-74^\circ 1569$	240	233 \pm 2	-8.5 ^a	152 \pm 2	-7.5 ^a	766 \pm 3	-137
R136a	260	167 \pm 2	+8	Blended	+7
		Blended	+224 [:]	Blended	+224 [:]
		Blended	+271 ^b	391 \pm 3 ^b	+271 ^b
30 Dor No. 11	90	168 \pm 3	+7	Blended	(+7)
		Blended	+273 ^b	711 \pm 5	{ +243: +270: +298:

^a Line has an asymmetric extended blue wing (see Fig. 2).

^b Feature is a blend of at least three components.

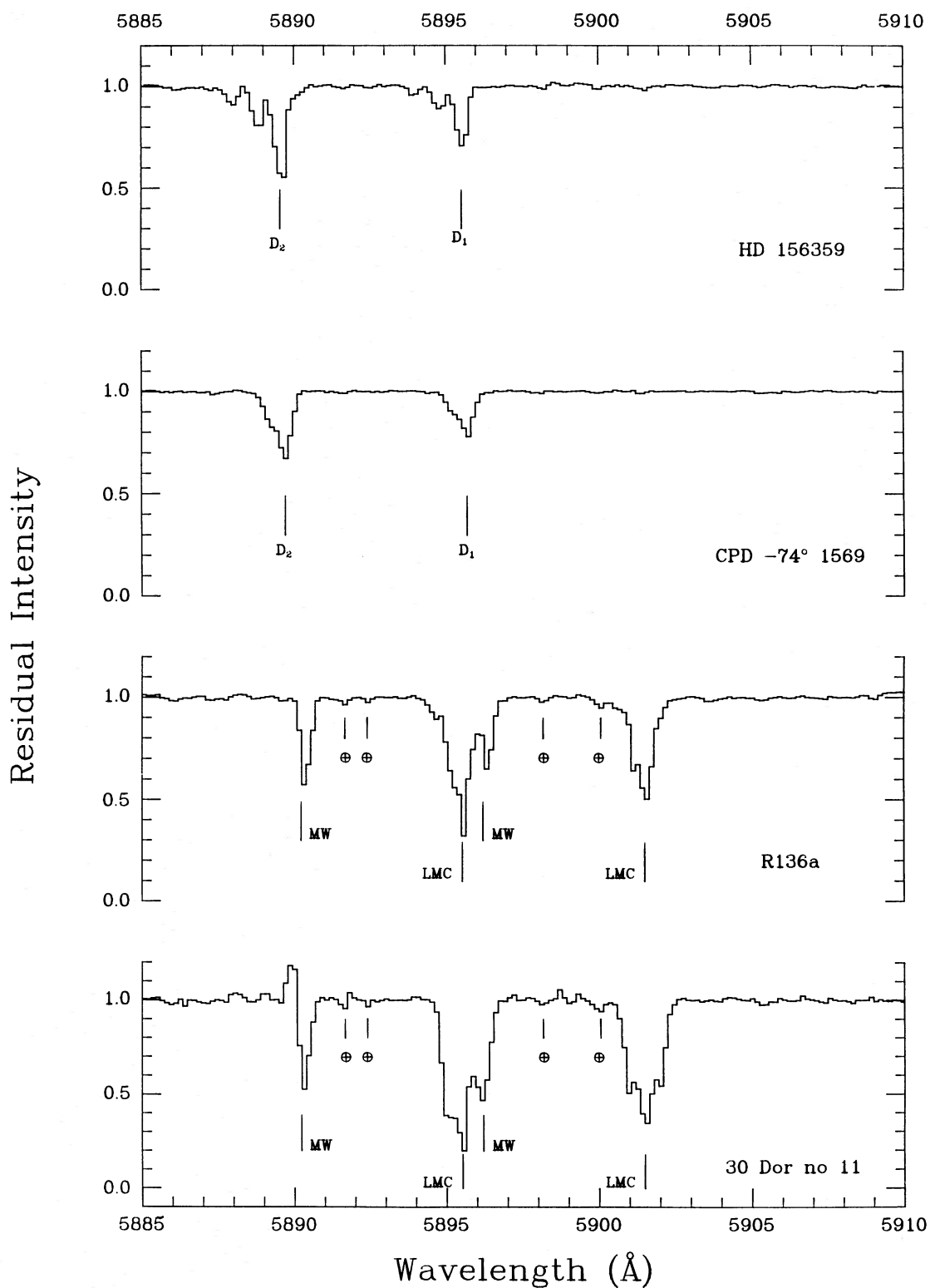


FIG. 2—Normalized profiles of the interstellar Na I lines in the four directions observed. The rest wavelengths ($v_{\text{LSR}}=0 \text{ km s}^{-1}$) of $\lambda 5889.950$ (D_2) and $\lambda 5895.924$ (D_1) are indicated by tick marks in the upper two panels. In each of the two lower panels two sets of tick marks indicate the expected positions of the doublet lines arising in quiescent neutral gas in the Milky Way ($v_{\text{LSR}}=0 \text{ km s}^{-1}$) and in the Large Magellanic Cloud ($v_{\text{LSR}}=+270 \text{ km s}^{-1}$). The symbols \oplus mark the strongest telluric water vapor features in the wavelength region of interest. The full scale of the ordinates shows to best advantage the high signal-to-noise ratios achieved in these observations, which, however, are of somewhat lower photometric accuracy than the [Fe x] data in Fig. 1, since the Na I lines fall in a less favorable position in the echelle blaze function (see Tables 2 and 4).

of these were excluded in the continuum-fitting procedure. We now comment briefly on each Na I profile in turn.

a) Stars in the Galactic Halo

The Na I lines in HD 156359 and CPD $-74^{\circ}1569$ both show a main component near zero velocity and additional, weaker absorption at negative velocities which, in HD 156359, is resolved into discrete components at $v_{\text{LSR}} = -37$ and $v_{\text{LSR}} = -81 \text{ km s}^{-1}$. The blue extent of the lines is probably a result of the spread of velocities produced by Galactic differential rotation over these two extended sight lines at intermediate latitudes. To illustrate this point, we show in Figure 3 the radial velocity expected in the direction of HD 156359, as a function of distance r from the Sun and z from the plane of the Galaxy, if the gas in the halo corotates with the disk. In this case, the velocities of the Na I components would imply cloud distances of, respectively, $r \approx 3$ and $r \approx 5.5 \text{ kpc}$ ($z \approx -0.8$ and $z \approx -1.4 \text{ kpc}$). However, these distances must be considered uncertain, since the clouds' velocities may include additional, random components, as well as a contribution from the large-scale velocity field of the Galaxy. The blue Na I components seen in HD 156359 are consistent with the complex profiles of the ultraviolet lines observed in this direction by Pettini and West (1982). Toward CPD $-74^{\circ}1569$ Galactic rotation produces a velocity curve similar to that in Figure 3, but with a smaller spread of velocities, and indeed the resulting Na I lines are clearly a blend of unresolved components distributed mainly over negative velocities. Interstellar Na I observations in this star, obtained with the image photon counting system at the Anglo-Australian Telescope have been previously reported by Keenan *et al.* (1983); the equivalent widths measured by these authors are in broad agreement with our values, within their quoted uncertainties of $\sim \pm 20\%$.

b) Stars in 30 Doradus

The interpretation of the Na I profiles toward 30 Dor is somewhat complicated by the fact that the wavelength separation of the doublet lines is comparable to the velocity difference between the Sun and this region of the LMC ($\sim 255 \text{ km s}^{-1}$; Smith and Weedman 1972), so that, at our resolution of 17 km s^{-1} , D_1 absorption by Milky Way gas is blended with D_2 components in the LMC (see bottom two panels of Fig. 2). Higher resolution ($5\text{--}8 \text{ km s}^{-1}$) observations of R136a by Blades (1980) and by Walborn (1980) have revealed that in this direction Na I absorption due to LMC gas consists of four components at $v_{\text{LSR}} = +227, +251, +271,$ and $+290 \text{ km s}^{-1}$ ($v_{\text{LSR}} = v_{\text{HELIO}} - 15.2 \text{ km s}^{-1}$). These components, although blended, can in fact be recognized in our Na I profiles for R136a in Figure 2, especially in the D_1 line, which is free from overlapping Galactic absorption. In particular, the high signal-to-noise ratio of the present data confirms the reality of the weakest component ($v_{\text{LSR}} \approx +227 \text{ km s}^{-1}$), which was not reported by Blades and is only marginally distinguishable above the noise in Walborn's spectrum.

A particularly interesting (and new) element of our observations is the comparison of the Na I profiles in R136a with those seen in front of star 11 in 30 Dor, separated by only $\sim 13.5 \text{ pc}$. While the agreement between the Galactic D_2 line in the two directions is excellent, LMC Na I absorption in the latter direction is almost twice as strong as in R136a and apparently consists of at least three components at $v_{\text{LSR}} \approx +243, +270,$ and $+298 \text{ km s}^{-1}$ (see Fig. 2 and Table 4). The increase appears to be due mainly, if not exclusively, to the two outer components ($v_{\text{LSR}} = +243$ and $+298 \text{ km s}^{-1}$), whose relationship to those seen in front of R136a cannot be established with the present resolving power. What is clear is that the gas they trace has a very patchy distribution, unlike the $v_{\text{LSR}} = +270$

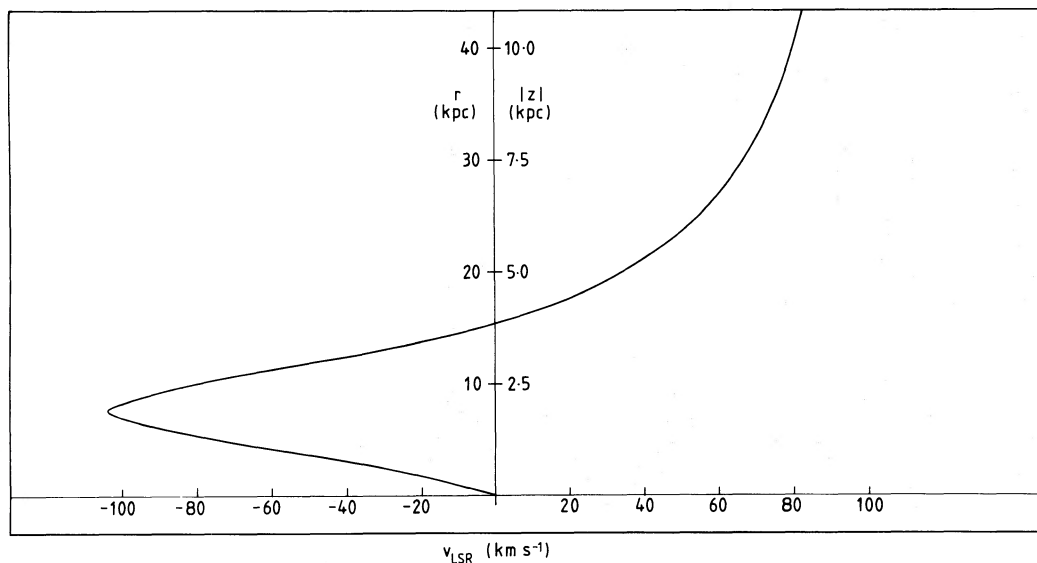


FIG. 3.—Run of velocities with distance from the Sun, r , and distance below the plane, z , produced by differential Galactic rotation in the direction of HD 156359 ($l = 328^{\circ}7, b = -14^{\circ}5$). The star itself is located at $r = 9 \text{ kpc}$ ($z = -2.2$). The velocities plotted correspond to a flat rotation curve for disk gas, with $v = 220 \text{ km s}^{-1}$ at galactocentric distances $R > 4 \text{ kpc}$, the Sun's galactocentric distance being taken to be $R_{\odot} = 8.7 \text{ kpc}$ (Gunn, Knapp, and Tremaine 1979; Savage and de Boer 1981). Furthermore, the curve shown assumes that gas in the halo corotates with the disk. A decrease in rotational velocity with distance z from the plane would result in a less pronounced spread of velocities along the line of sight. If the velocities of the Na I components seen in front of HD 156359 are due to Galactic rotation, the corresponding cloud distances are, respectively, $r \approx 3$ and $r \approx 5.5 \text{ kpc}$ ($z = -0.8$ and $z = -1.4 \text{ kpc}$).

km s⁻¹ component, which, according to the detailed study of the spatial structure of the gas in 30 Dor by de Boer, Koornneef, and Savage (1980), constitutes a more widespread foreground region, where most of the neutral gas and dust in front of 30 Dor are located. Our Na I observations, and the detection of the diffuse interstellar bands $\lambda\lambda 6376.08, 6379.30$ at $v_{\text{LSR}} = +269$ km s⁻¹, support this interpretation. It is interesting to note that the two components at $v_{\text{LSR}} = +243$ and $v_{\text{LSR}} = +298$ km s⁻¹ seen in 30 Dor No. 11 are symmetrically spaced in velocity from the foreground H I gas at $v_{\text{LSR}} = +270$ km s⁻¹. Thus, we may have detected *both* halves of a shell, located in front of the star and expanding at ~ 28 km s⁻¹ relative to the ambient medium. The relationship, if any, of this shell to other interstellar line components and to the expanding H II region seen in emission (Smith and Weedman 1972; Walborn

1980), can be investigated only with a detailed survey of the gas in 30 Dor at both high resolution and high signal-to-noise ratio. The new short camera of the coude echelle spectrograph of the 1.4 m coude auxiliary telescope at ESO, now equipped with a 15 μ m pixel RCA CCD chip giving a resolving power of $\sim 70,000$ (Dekker *et al.* 1986), offers the opportunity of carrying out this interesting set of observations in the near future.

We are grateful to Tom Hartquist, Ted Snow, and Pete Storey for useful discussions, and to Klaas de Boer for communicating unpublished data. Dave L. King and Monica Everest at RGO kindly produced the figures for this paper. Max Pettini would like to acknowledge the generous hospitality of the European Southern Observatory in Munich, where this work was completed.

REFERENCES

- Bergeron, J. 1986, *Astr. Ap.*, **155**, L8.
 Blades, J. C. 1980, *M.N.R.A.S.*, **190**, 33.
 Blades, J. C., and Madore, B. F. 1979, *Astr. Ap.*, **71**, 359.
 Bregman, J. N. 1980, *Ap. J.*, **236**, 577.
 Bregman, J. N., and Harrington, P. J. 1986, *Ap. J.*, **309**, 833.
 Bromage, G. E., and Nandy, K. 1983, *M.N.R.A.S.*, **204**, 29P.
 Crawford, M. K., Tielens, A. G. G. M., and Allamandola, L. J. 1985, *Ap. J. (Letters)*, **293**, L45.
 de Boer, K. S. 1984, in *Proc. Fourth European IUE Conference* (ESA SP-218), p. 179.
 de Boer, K. S., Fitzpatrick, E. L., and Savage, B. D. 1985, *M.N.R.A.S.*, **217**, 115.
 de Boer, K. S., Koornneef, J., and Savage, B. D. 1980, *Ap. J.*, **236**, 769.
 de Boer, K. S., and Nash, A. G. 1982, *Ap. J.*, **255**, 447.
 de Boer, K. S., and Savage, B. D. 1980, *Ap. J.*, **238**, 86.
 Dekker, H., Delabre, B., D'Odorico, S., Lindgren, H., Maaswinkel, F., and Reiss, R. 1986, *ESO Messenger*, **43**, 27.
 D'Odorico, S., Pettini, M., and Ponz, D. 1985, *Ap. J.*, **299**, 852.
 D'Odorico, S., and Tanné, J. F. 1984, *ESO Operating Manual*, No. 2.
 Feast, M. W. 1961, *M.N.R.A.S.*, **122**, 1.
 Feitzinger, J. V., Schlosser, W., Schmidt-Kaler, Th., and Winkler, C. 1980, *Astr. Ap.*, **84**, 50.
 Fitzpatrick, E. L., and Savage, B. D. 1984, *Ap. J.*, **279**, 578.
 Fransson, C., and Chevalier, R. A. 1985, *Ap. J.*, **296**, 35.
 Gunn, J. E., Knapp, G. R., and Tremaine, S. D. 1979, *A.J.*, **84**, 1181.
 Hartquist, T. W., Pettini, M., and Tallant, A. 1984, *Ap. J.*, **276**, 519.
 Herbig, G. H. 1975, *Ap. J.*, **196**, 129.
 Hobbs, L. M. 1984a, *Ap. J.*, **280**, 132.
 ———. 1984b, *Ap. J. (Letters)*, **284**, L47.
 ———. 1985, *Ap. J.*, **298**, 357.
 Houziaux, L., Nandy, K., and Morgan, D. H. 1980, *Astr. Ap.*, **84**, 377.
 Hutchings, J. B. 1980, *Pub. A.S.P.*, **92**, 592.
 Jenkins, E. B. 1984, in *IAU Colloquium 81, The Local Interstellar Medium*, ed. Y. Kondo, F. C. Bruhweiler, and B. D. Savage (NASA Conf. Pub. 2345), p. 155.
 Kahn, F. D. 1976, *Astr. Ap.*, **50**, 145.
 Keenan, F. P., Dufton, P. L., McKeith, C. D., and Blades, J. C. 1983, *M.N.R.A.S.*, **203**, 963.
 Koornneef, J., and Code, A. D. 1981, *Ap. J.*, **247**, 860.
 Krishna Kumar, C., Federman, S. R., and Vanden Bout, P. A. 1982, *Ap. J. (Letters)*, **261**, L51.
 Kroto, H. W., Heath, J. R., O'Brien, S. C., Curl, R. F., and Smalley, R. E. 1985, *Nature*, **318**, 162.
 Long, K. S., Helfand, D. J., and Grabelsky, D. A. 1981, *Ap. J.*, **248**, 925.
 Mathis, J. S., and Wallenhorst, S. G. 1981, *Ap. J.*, **244**, 483.
 McKee, C. F., and Cowie, L. L. 1977, *Ap. J.*, **215**, 213.
 Melnick, J. 1985, *Astr. Ap.*, **153**, 235.
 Merrill, P. W. 1934, *Pub. A.S.P.*, **46**, 206.
 Nandy, K. 1984, in *IAU Symposium 108, Structure and Evolution of the Magellanic Clouds*, ed. S. van den Bergh and K. S. de Boer (Dordrecht: Reidel), p. 341.
 Pettini, M., and Bokseberg, A. 1987, *Ap. J.*, submitted.
 Pettini, M., and West, K. A. 1982, *Ap. J.*, **260**, 561.
 Ponz, D., Brinks, E., and D'Odorico, S. 1986, *Proc. SPIE*, **267**, in press.
 Reid, I. N., and Strugnell, P. R. 1986, *M.N.R.A.S.*, in press.
 Savage, B. D. 1985, in *Proc. Green Bank Workshop, The Gaseous Halos of Galaxies* (Wisconsin Ap. Preprint, No. 229).
 Savage, B. D., and de Boer, K. S. 1981, *Ap. J.*, **243**, 460.
 Savage, B. D., and Massa, D. 1985, *Ap. J. (Letters)*, **295**, L9.
 Seab, C. G., and Snow, T. P. 1984, *Ap. J.*, **277**, 200.
 Shapiro, P. R., and Holcomb, K. A. 1986, *Ap. J.*, **305**, 433.
 Shull, J. M., and Van Steenberg, M. 1982, *Ap. J. Suppl.*, **48**, 95.
 Smith, M. G., and Weedman, D. W. 1972, *Ap. J.*, **172**, 307.
 Smith, W. H., Snow, T. P., Jura, M., and Cochran, W. D. 1981, *Ap. J.*, **248**, 128.
 Snow, T. P., and Cohen, J. G. 1974, *Ap. J.*, **194**, 313.
 Snow, T. P., Timothy, J. G., and Saar, S. 1982, *Ap. J.*, **262**, 611.
 Spitzer, L., Jr. 1956, *Ap. J.*, **124**, 20.
 Spitzer, L., Cochran, W. D., and Hirshfeld, A. 1974, *Ap. J. Suppl.*, **28**, 373.
 Walborn, N. R. 1977, *Ap. J.*, **215**, 53.
 ———. 1980, *Ap. J. (Letters)*, **235**, L101.
 ———. 1984, in *IAU Symposium 108, Structure and Evolution of the Magellanic Clouds*, ed. S. van den Bergh and K. S. de Boer (Dordrecht: Reidel), p. 243.
 Weigelt, G., and Baier, G. 1985, *Astr. Ap.*, **150**, L18.
 Welter, G. L., and Savage, B. D. 1977, *Ap. J.*, **215**, 788.
 Withbroe, G. L. 1971, in *The Menzel Symposium*, ed. K. B. Gebbie (NBS Spec. Pub. 353).
 Wu, C.-C., York, D. G., and Snow, T. P. 1981, *A.J.*, **86**, 755.
 York, D. G. 1982, *Ann. Rev. Astr. Ap.*, **20**, 221.
 York, D. G., and Cowie, L. L. 1983, *Ap. J.*, **264**, 49.

SANDRO D'ODORICO: European Southern Observatory, Karl-Schwarzschild-Strasse 2, D-8046 Garching-bei-München, Federal Republic of Germany

MAX PETTINI: Royal Greenwich Observatory, Herstmonceux Castle, Hailsham, East Sussex, BN27 1RP, UK